

****FULL TITLE****

*ASP Conference Series, Vol. **VOLUME**, **YEAR OF PUBLICATION***

****NAMES OF EDITORS****

Turbulence Effects at Small Scales

A. Beresnyak and A. Lazarian

Astronomy Department, University of Wisconsin-Madison, 475 Charter St., Madison, WI 53705

Abstract. It is most natural to assume that mysterious Small Ionized and Neutral Structures (SINS) in diffuse ISM arise from turbulence. There are two obvious problem with such an explanation, however. First of all, it is generally believed that at the small scales turbulence should be damped. Second, turbulence with Kolmogorov spectrum cannot be the responsible for the SINS. We consider, however, effects, that provide spectral index flatter than the Kolmogorov one and allow action at very small scales. These are the shocks that arise in high Mach number turbulence and transfer of energy to small scales by instabilities in cosmic rays. Our examples indicate that the origin of SINS may be discovered through systematic studies of astrophysical turbulence.

1. Turbulence and SINS

Various observations covered well in this volume indicate the existence of structure in the neutral and ionized ISM on AU spatial scales, causing concern about how well we understand the basics of the ISM physics. In the straightforward interpretation, these clouds should be extremely overdense and overpressured. Evaporation arguments point to very short lifetimes of such clouds, yet the AU-scale structures in the diffuse medium seem quite common. In this volume the reader can find many articles dealing with the observed properties of SINS. Therefore we do not dwell upon this issue. Instead we adopt a broad theoretical approach and ask a question whether turbulence can produce enough activity on small scales to be considered as a potential source of SINS.

The attractiveness of turbulence as an origin of SINS is that it can produce a generic universal explanation. Indeed, turbulence is really ubiquitous in astrophysics, including the ISM and circumstellar regions. However, the most popular Kolmogorov turbulence model can not account for SINS. Kolmogorov turbulence has a spectrum of $E(k) \sim k^{-5/3}$, the fluctuations of density at scale $k \sim 1/l$ arisen from advection by turbulence are $(\delta\rho_k)^2 \sim kE(k) \sim k^{-2/3}$, i.e. they decrease with the scale. SINS, on the contrary, are connected to rather large density contrasts at small scales. This would violate the assumption of Kolmogorov turbulence that it is only weakly compressive at large outer scale. Fortunately, astrophysical turbulence is not limited to the Kolmogorov spectrum. If the spectrum of density fluctuations scales as $E(k) \sim k^{-n}$, $n < 1$, then $(\delta\rho_k)^2$ increases with the decrease of turbulence scale.

As we see from the example above, in terms of turbulence, the origin of SINS is a quantitative question related to the spectra of turbulent motions. This question cannot be dealt using brute force of computers. Indeed, from

the point of view of fluid mechanics astrophysical turbulence is characterized by huge Reynolds numbers, Re , which is the inverse ratio of the eddy turnover time of a parcel of gas to the time required for viscous forces to slow it appreciably. For $Re \gg 100$ we expect gas to be turbulent and this is exactly what we observe in HI (for HI $Re \sim 10^8$). In fact, very high astrophysical Re and its magnetic counterpart magnetic Reynolds number Rm (that can be as high as $Rm \sim 10^{16}$) present a big problem for numerical simulations that cannot possibly get even close to the astrophysically-motivated numbers¹. The currently available 3D simulations can have Re and Rm up to $\sim 10^4$. Both scale as the size of the box to the first power, while the computational effort increases as the fourth power (3 coordinates + time), it is not feasible to resolve the actual interstellar turbulent cascade to test whether SINS somehow emerge at the end of it. Another approach based on (a) establishing scaling relations that can be tested with the modern computers and (b) testing these relations with observational data seems promising. In what follows we discuss the part (a). Part (b) is addressed in a recent review by Lazarian (2006).

2. Density spectrum in supersonic MHD turbulence

A very important insight into the incompressible MHD turbulence by Goldreich & Shridhar (1995) (henceforth GS95) has been followed by progress in understanding of compressible MHD turbulence (Lithwick & Goldreich 2001, Cho & Lazarian 2003, henceforth CL03, Cho, Lazarian & Vishniac 2003). In particular, simulation in Cho & Lazarian (2003) showed that Alfvénic cascade evolves on its own² and it exhibits Kolmogorov type scaling (i.e. $E \sim k^{-5/3}$) and scale-dependent anisotropy of the Goldreich-Shridhar type (i.e. $k_{\parallel} \sim k_{\perp}^{2/3}$) even for high Mach number turbulence. While slow modes exhibit similar scalings and anisotropy, fast modes show isotropy. The density scaling obtained in Cho & Lazarian (2003) was somewhat puzzling. At low Mach numbers it was similar to slow modes, while it got isotropic for high Mach numbers.

Density power spectrum shallower than the Kolmogorov one was reported in a number of observations (Deshpande, Dwarakanath & Goss 2000, Padoan et al 2003) and the relation between the SINS and the shallow power spectrum was advocated in Deshpande (2000).

For high Mach numbers we expect shocks to develop; the density should be perturbed most dramatically by those shocks. Naively, one would think that density perturbations will have a random-shock spectrum of k^{-2} which leaves very little perturbation on small scales. Also, in sub-Alfvénic turbulence magnetic field is dynamically important, so we expect to observe some anisotropy

¹This caused serious concerns that while present codes can produce simulations that resemble observations, whether numerical simulations reproduce reality well (see McKee 1999, Shu et al. 2004).

²The expression proposed and tested in CL03 shows that the coupling of Alfvénic and compressible modes is appreciable at the injection scale if the injection velocity is comparable with the *total* Mach number of the turbulence, i.e. with $(V_A^2 + C_S^2)^{1/2}$, where V_A and C_S are the Alfvén and sound velocities respectively. However, the coupling gets marginal at smaller scales as turbulence cascades and turbulent velocities get smaller.

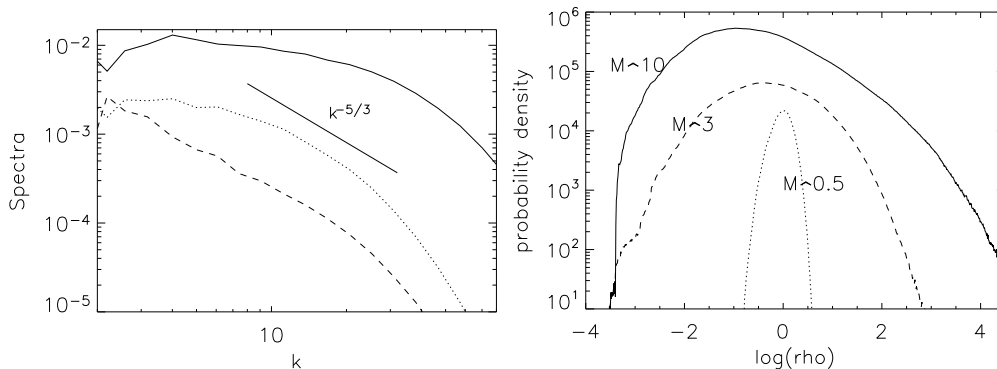


Figure 1. *Left panel:* Mach number is 10, power spectra of: *solid* – density, *dashed* – velocity, *dotted* – logarithm of density. *Right Panel:* Probability density function for a density in simulation with Alfvénic Mach number around unity and various sonic Mach numbers.

which is typical for magnetic turbulence. None of these two properties is actually observed in simulations. On the contrary, the spectrum was typically rather shallow and there was no significant anisotropy. This mystery is resolved as follows: shocks in isothermal fluid can have very large density contrasts, up to sonic Mach squared, however the conservation of mass and positive sign of density allows only small regions with high-density or clumps. These clumps totally dominate the spectrum of density. Being close to delta-functions, they generate rather shallow spectrum. Being distributed randomly in space, they mask any anisotropy originally present due to Alfvénic shearing.

Our calculations in Beresnyak, Lazarian & Cho (2006, henceforth BLC06) demonstrated that the spectrum of density for high Mach number MHD turbulence is shallow (see Fig. 1). This potentially may be important for SINs, although we do not attempt to provide quantitative arguments for this at the present stage. The rms deviation of density for a subsonic case is consistent with prediction M^2 for low beta (CL03), and the rms deviation of log-density for supersonic case is around unity regardless of a Mach number. The distributions are notably broader for higher Mach numbers, though.

Dimension of the high-density structures is between 1 and 2, being viewed as a flatted filaments or elongated pancakes. There were no evident preferred orientation of these structures along or perpendicular to the mean magnetic field. Maximum density value in a Mach 10 data cube was around $3 \times 10^3 \rho_0$. We also noted in BLC06 that the randomly distributed high-density clumps suppress any anisotropy originating from motions at small scales.

In magnetically dominated medium that we deal with it is reasonable to assume that the corresponding shocks move material along magnetic field lines the same way that the slow modes do in subsonic case. The shocks are randomly oriented and therefore the clumpy structure that we observe does not reveal any noticeable anisotropy. In fact, the density perturbations associated with such shocks should not be correlated with the magnetic field strength enhancement, which our data analysis confirms. Note, that due to different reasons, this

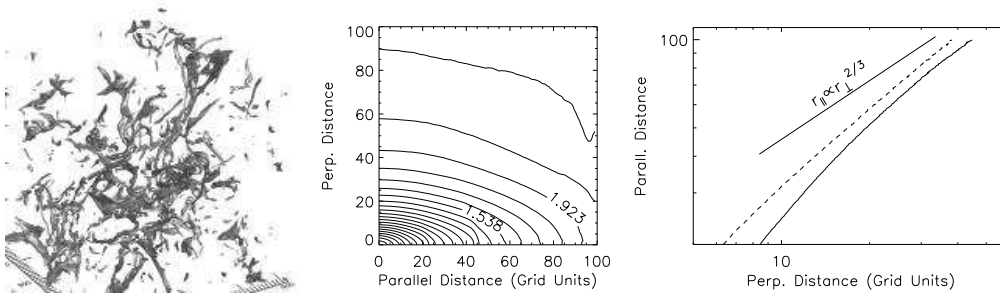


Figure 2. $M_s \sim 10$, *Left Panel*: The isosurfaces of density, corresponding to 10 mean densities. *Central Panel*: Contours of equal correlations of log-density, calculated respective to the local magnetic field. They reveal pronounced anisotropy of density structure. *Right panel*: r_{\parallel} and r_{\perp} for anisotropic eddies revealed by logarithm of density, and comparison with GS95 law, *solid* $M_s \sim 10$, *dashed* $M_s \sim 3$.

correlation also weak for density fluctuations induced by slow modes low Mach number MHD turbulence (see CL03).

Interestingly enough, similar results in terms of shallow density spectrum are seen in pure high Mach number hydrodynamic simulations (Kim & Ryu 2005). This reinforces the idea that the primary mechanism for generating of flat spectrum of density is the random multiplication/division of density in supersonic flows which, together with mass conservation, form isolated high peaks of density. Does this mean that magnetic field is totally unimportant for the structure of density in supersonic turbulence? Not at all – we were able to reveal the underlying density structure, that comes from Alfvénic shearing by using a log-density instead of density for spectra and structure functions. The structure function of log-density have shown very familiar Goldreich-Sridhar scale-dependent anisotropy, typical for almost any quantity in sub-Alfvénic compressible turbulence (see Fig. 2).

Calculations of the density scaling with a more extended sample of simulations with a variety of ordinary and Alfvén Mach numbers in Kowal, Lazarian & Beresnyak (2006) are consistent with our findings above. The explanation of the shallow spectrum of density presented above suggests that if we include gravity the clumps will be denser and the power spectrum of density will be flatter or could be even rising (δ -functions will give the 1D power spectrum of k^2)

In terms of the relation to SInS, we may note, that cooling may make interstellar gas more pliable to compression than the isothermal gas that we used in the simulations. This, could result in more density contrast when the original gas is warm. This calls for detailed studies that include cooling.

3. Alfvénic Slab motions induced by Cosmic Rays

In this section we describe a new mechanism to transfer turbulent energy to small scales bypassing the usual turbulent cascade. This mechanism, described in Lazarian & Beresnyak (2006) allow us to have relatively large-amplitude slab-type Alfvénic perturbations on small scales. Even though MHD Alfvén waves do

not perturb density, small-scale kinetic Alfvén waves (KAW) do. Also the slab Alfvén waves in a compressible media is subject to the well-known parametric instability that produces density perturbations.

The close connection between the cosmic ray (CR) power-law and the turbulence power-law is the point that was stressed by Randy Jokipii in many of his presentations (see Jokipii 2001). The physical essence of this relation and, in fact, the very understanding of the interaction of CR and turbulence are currently the issues of intensive research. It is well known that the propagation of CR depends on the scaling of the ISM turbulence. Most of the studies in the field use isotropic or slab-like Alfvénic turbulence the origin of which does not follow from either theoretical models of MHD turbulence (see Goldreich & Shridhar 1995; review by Cho & Lazarian 2005 and references therein) or numerical simulations of MHD turbulence (see Cho & Lazarian 2003 and references therein). On the contrary, the interactions of Alfvénic turbulence with scale dependent anisotropy that is consistent with both theoretical predictions and numerics were shown to be inefficient for cosmic ray scattering (Chandran 2000, Yan & Lazarian 2002). Using the scalings for fast modes obtained in Cho & Lazarian (2003), Yan & Lazarian (2002) identified fast modes as the principal scattering agent for standard models of MHD turbulence, provided that the energy is injected at scales larger than a pc. In this model that follows from this work the differences in damping of fast modes result in the differences in CR propagation in different ISM phases. This induces substantial changes on the models of CR propagation in our galaxy (Yan & Lazarian 2004) and in clusters of galaxies (Brunetti & Lazarian 2006).

While the above changes of the picture of CR propagation and possibly acceleration are inevitable in the quasi-linear models of scattering by MHD turbulence injected at large scales, in an astrophysically realistic situation with the pressure of CRs close to thermal or magnetic pressure, it is reasonable to ask whether the feedback of CRs to MHD turbulence is important. This question was addressed in Lazarian & Beresnyak (2006). CRs react very differently from ordinary gas when the magnetized fluid is compressed, if the scale of compression is less than CR mean free path. Such scale compressions or expansions change only the component of CR momentum that is perpendicular to magnetic field (due to the so-called “adiabatic invariant” conservation), while the component of the momentum parallel to magnetic field stays the same. Such state is, however, unstable.

We calculated the rate of CR kinetic instability that transfers energy to small scales, creating small-scale Alfvénic perturbations that are not a part of the global MHD cascade. These perturbations are more like waves moving along magnetic field lines and thus are very different from highly anisotropic GS95 Alfvénic modes.

Quantitatively, we consider a power-law distribution of CRs $F_0 \sim p^{-\alpha-2}$ where α is conveniently defined as the power-law index for a one-dimensional distribution (or particle density). For example, around the Earth $\alpha \sim 2.6$ up to the energies of 10^{14} eV. The growth rate of the cosmic-ray-Alfvén gyroresonance instability (henceforth GI) can be estimated as:

$$\gamma_{\text{CR}}(k_{\parallel}) = \pm \omega_{pi} \frac{n_{\text{CR}}(p > m\omega_B/k_{\parallel})}{n} A Q, \quad (1)$$

where $n_{\text{CR}}(p > m\Omega/k_{\parallel})$ is the number density of CRs with momentum larger than the minimal resonant momentum for a wave vector value of k_{\parallel} , m is the proton mass, n is the density of the thermal plasma, ω_{pi} is the ion plasma frequency. Q is a numerical factor that depends on the index of cosmic rays α . The \pm sign corresponds to the two MHD modes. We shall concentrate on the Alfvén mode, corresponding to the plus sign, as those are less subjected to linear damping. We show that when anisotropy is created by compressive turbulence, the anisotropy factor $A = (p_{\perp} - p_{\parallel})/p_{\parallel}$ is small and changes its sign on the scale of the mean free path, depending on two competitive mechanisms – scattering which tends to isotropize momentum distribution, and magnetic field compression which tends to make it oblate or prolate.

Assuming that anisotropy arises from the turbulent compressions with amplitude δv at large scale, the factor A is equal to $2\delta v/v_A$, where v_A is the Alfvén velocity. Then the expression for the instability rate can be written as

$$\gamma_{\text{CR}}(r_p) = \frac{\delta v}{L_i} \left(\frac{r_p}{r_0} \right)^{-\alpha+1}, \quad (2)$$

where r_p is a Larmor radius of a CR resonant with a particular wave vector $k_{\parallel} = m\Omega/p$, r_0 is the 1 GeV proton Larmor radius and

$$L_i = 3.7 \cdot 10^{-7} \frac{1}{Q} \left(\frac{B}{5 \cdot 10^{-6} \text{ G}} \right) \left(\frac{4 \cdot 10^{-10} \text{ cm}^{-3}}{n_{\text{CR}}(r_p > r_0)} \right) \text{ pc}. \quad (3)$$

This CR instability gets energy from external turbulent compressions of CR at the mean free path scale and directly transfers it to scale of the CR Larmor radius.

There are two non-linear processes limit the growth rate of the instability. First of all, the magnetic perturbations generated at the Larmor radius of CR backreact on CR by limiting the mean free path λ . If the change of magnetic field direction is $\phi \sim \delta B/B$ the scattering that is a random walk requires $N \sim 1/\phi^2$ interaction and

$$\lambda \sim Nr_p \sim r_p/\phi^2 \sim r_p B^2/(\delta B)^2, \quad (4)$$

where we designated δB as the magnetic field perturbation pertaining to a particular wavenumber, i.e. $\delta B^2 \approx E(k)k$. We can consider δB as a function of either k or the resonant Larmor radius r_p (see Longair 1994). δB grows as the instability grows, which in turn reduces λ . On the other hand, it is the mean free path λ which determines the scale at which compressions of the magnetic field are important. This can be understood as follows: the CR distribution “remembers” the perturbed value of the magnetic field and its anisotropy only during the time the typical particle travels its mean free path. Once particles scatter significantly, the anisotropy of the distribution is effectively “reset”. As a result only low amplitude motions on scales less than λ excite the instability which limits the degree of anisotropy A attainable.

The instability grows as $d(\delta B^2)/dt = \gamma_{\text{CR}}(\delta B^2)$ where the injection of energy is happening at the scale of the mean free path, i.e.

$$\gamma_{\text{CR}} \approx \frac{v_A}{L_i} \left(\frac{r_p}{L} \right)^{\mu} \left(\frac{\delta B}{B} \right)^{-2\mu} \left(\frac{r_p}{r_0} \right)^{-\alpha+1}, \quad (5)$$

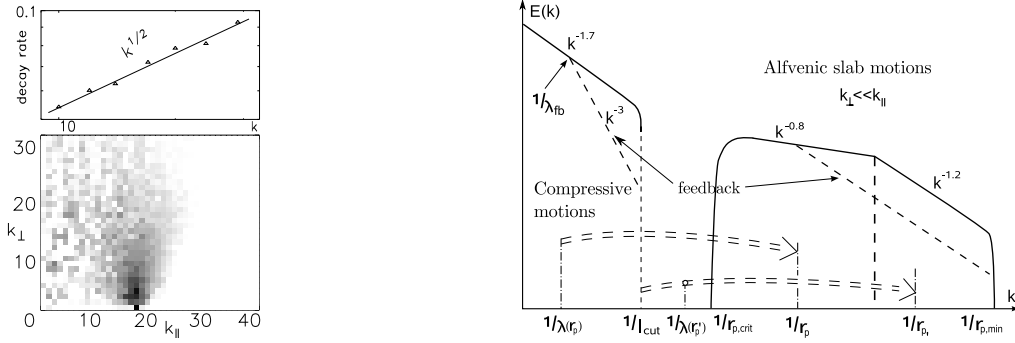


Figure 3. *Left Panel:* Decorrelation of a plane, $k_{\perp} = 0$ Alfvén wave by turbulence. Lower picture shows the energy density of a wave in cylindrical k -space. Alfvén waves were injected at $k_{\parallel} = 17$. Wave energy is being transferred in the direction of k_{\perp} axis, which is typical for decorrelation by MHD turbulence. Upper plot shows decay rate of the wave vs its wavenumber. *Right Panel:* Energy density of compressive modes and Alfvénic slab-type waves, induced by CRs. The energy is transferred from the mean free path scale to the CR Larmor radius scale. If the mean free path falls below compressive motions cutoff or feedback suppression scale, the spectrum of slab waves becomes steeper. See more on feedback in Lazarian & Beresnyak (2006).

where eqs. (2) and (4) were used. We see that according to the above equations δB perturbations will grow as $t^{1/2\mu}$ thus reducing λ virtually to r_p . If not for other processes, it is possible to show that this suppression would reduce λ to virtually the CR gyroradius, inducing Bohm-type diffusion of CRs.

However, the collection of waves with different wavelengths created by the instability is also subject to steepening with the rate of $\gamma_{\text{steep}} \approx -(\delta B/B)^2 k_{\parallel} v_A$, which combined with the effect of limiting λ above provides:

$$\frac{\delta B}{B} \approx \frac{r_0^{1/2}}{L_i^{1/(2\mu+2)} L^{\mu/(2\mu+2)}} \left(\frac{r_p}{r_0} \right)^{(\mu-\alpha+2)/(2\mu+2)}. \quad (6)$$

For $\alpha = 2.6$ and $\mu = 1/3$ Eq. (6) produces a rather shallow spectrum of perturbations, $E(k) \approx (\delta B)^2/k \sim k^{-0.8}$.

The calculations above are valid provided that λ is larger than the compressive mode cutoff scale l_{cut} . If, on the other hand, $l_{\text{cut}} > \lambda$ the compression for the instability is supplied from the eddies at the damping scale, namely, $\delta v/v_A \sim (l_{\text{cut}}/L)^{1/3}(\lambda/l_{\text{cut}})$. In this case instead of eq. (6) one gets

$$\frac{\delta B}{B} \approx \left(\frac{r_0^{1/2}}{L_i^{1/4} L^{\mu/4} l_{\text{cut}}^{(1-\mu)/4}} \right)^{1/4} \left(\frac{r_p}{r_0} \right)^{(3-\alpha)/4}, \quad (7)$$

which, for the same value of $\alpha = 2.6$, corresponds to a steeper spectrum of $E(k) \sim k^{-1.2}$.

The ambient Alfvénic turbulence provides yet another source of non-linear damping of the waves generated by the instability. This process is analogous to the suppression of the streaming instability (Yan & Lazarian 2002, Farmer

& Goldreich 2004). Our numerical testings of the scalings of the corresponding damping rate, i.e.

$$\gamma_{\text{turb}} \sim -k_{\perp} v_{\perp} \sim -v_A k_{\perp}^{2/3} L^{-1/3} \sim -v_A r_p^{-1/2} L^{-1/2}, \quad (8)$$

are shown in Figure 3 (left). The encouraging agreement of Eq. 8 with the results of MHD simulations makes us confident in using this rate, which up to the sign convention, coincides with the prediction in Farmer & Goldreich (2004). Combining eqs. (5), (6) and (8) we find that for $\alpha > 5/3$ our instability is damped for all scales, larger than

$$r_{p,\text{crit}} \approx r_0 \left(L^{1-\mu} r_0^{\mu+1} L_i^{-2} \right)^{1/(2\alpha-\mu-3)}. \quad (9)$$

Therefore the spectrum of plane Alfvén waves given by eq. (6) will protrude from $r_{p,\text{crit}}$ down to $r_{p,\text{min}}$ which corresponds to minimum energies of CRs.

4. Summary

Astrophysicists always expect to see Kolmogorov turbulence. These expectations may not be met in reality. We presented two examples of astrophysical processes that provide distinctly non-Kolmogorov spectra. One case is the density in supersonic MHD turbulence, another is the velocity and magnetic field perturbations at small scales. This work is suggestive that a possible explanation of the SINS should be sought invoking non-Kolmogorov turbulence.

Acknowledgments. AB thanks IceCube project for support of his research. AL acknowledges the NSF grant AST-0307869 and the support from the Center for Magnetic Self-Organization in Laboratory and Astrophysical Plasmas.

References

- Beresnyak, A., Lazarian, A. & Cho, J. 2005, *ApJ*, **640**, L175
 Brunetti, G. & Lazarian, A. 2006, *MNRAS*, submitted
 Chandran B.D.G. 2000, *Phys. Rev. Lett.*, **85** (22), 4656-4659
 Cho, J. & Lazarian, A. 2003, *MNRAS*, **345**, 325
 Cho, J. & Lazarian, A. 2005, *Theor. and Comput. Fluid Dynamics*, **19**, 127-157
 Cho, J., Lazarian, A., & Vishniac, E. 2003, *ApJ*, **595**, 812-823
 Deshpande, A.A. 2000, *MNRAS*, **317**, 199
 Deshpande, A.A., Dwarakanath, K.S., Goss, W.M., 2000, *ApJ*, **543**, 227-234
 Farmer, A., & Goldreich, P. 2004, *ApJ*, **604**, 671
 Goldreich, P. & Sridhar, S. 1995, *ApJ*, **438**, 763
 Jokipii, R. 2001, ASP Conf. Proc. Vol. 241, ed. C. Ko, p. 223
 Kowal, G., Lazarian, A. & Beresnyak, A. 2006, *ApJ*, submitted
 Lazarian, A. in Spectral line Shapes, AIP, in press, astro-ph/0610765
 Lazarian, A. & Beresnyak, A. 2006, *MNRAS*, in press
 Lithwick, Y. & Goldreich, P. 2001, *ApJ*, **562**, 279
 McKee, C. 1999, in *The Origin of Stars and Planetary Systems*, ed. Charles J. Lada and Nikolaos D. Kylafis. Kluwer Academic Publishers, p.29
 Shu, F.H., Li, Z.-Y., & Allen, A. 2004, *ApJ*, **601**, 930
 Padoan, P., Goodman, A. & Juvela, M. 2003, *ApJ*, **588**, 308
 Yan, H. & Lazarian, A. 2002, *Phys. Rev. Lett.*, **89**, number 28, 1102
 Yan, H. & Lazarian, A. *ApJ*, **614**, 757